Agricultural and Forest Meteorology 362 (2025) 110370

Contents lists available at ScienceDirect

Agricultural and Forest Meteorology

journal homepage: www.elsevier.com/locate/agrformet

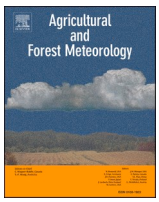

Reductions in nitrous oxide emissions in diverse crop rotations linked to changes in prokaryotic community structure

Mingming Zong [a,b,c,d], Xiaolin Yang [a,b,*], Alberto Sanz-Cobena [e,f], Uffe Jørgensen [c,d], Klaus Butterbach-Bahl [f,g], Diego Abalos [c,f]

[a] State Key Laboratory of Efficient Utilization of Agricultural Water Resources, China Agricultural University, Beijing 100083, PR China
[b] Center for Agricultural Water Research in China, China Agricultural University, Beijing 100083, PR China
[c] Department of Agroecology, Aarhus University, Tjele 8830, Denmark
[d] Centre for Circular Bioeconomy, Aarhus University, Tjele 8830, Denmark
[e] CEIGRAM, ETSI Agronomica, Alimentaria y de Biosistemas, Universidad Politécnica de Madrid, Madrid 28040, Spain
[f] Land-CRAFT, Department of Agroecology, Aarhus University, Aarhus 8000, Denmark
[g] Institute of Meteorology and Climate Research, Atmospheric Environmental Research (IMK-IFU), Karlsruhe Institute of Technology (KIT), Garmisch Partenkirchen 82467, Germany

ARTICLE INFO

Keywords:
Crop rotation
N_2O emissions
Emission factors
Prokaryotic functions functional predictions
Nitrification and denitrification

ABSTRACT

Diverse crop rotations are increasingly recognized as key to address the global food crisis and improve environmental sustainability, including reducing nitrous oxide (N_2O) emissions. However, the specific effects on N_2O emissions of different crops in these rotations and the underlying incidence on microbial processes remain underexplored. In a six-year field study, we compared N_2O emissions from traditional wheat-maize rotation with diverse rotations, including legumes (peanut, soybean), ryegrass, sorghum, and sweet potato. We also examined the microbial functions associated with nitrogen cycling based on functional annotation of prokaryotic taxa (FAPROTAX) analysis. Our study showed that diversified crop rotations with reduced synthetic fertilization and irrigation can reduce N_2O emissions by 23 %-49 % compared to conventional rotations. These reductions were supported by increases in soil organic carbon, soil carbon/nitrogen ratio and decreases in the relative abundance of denitrifying microorganisms, particularly observed in rotations with soybean and sweet potato. However, the spring maize and peanut-based rotation had higher emission factors than traditional wheat-maize rotation due to lower initial crop nitrogen uptake and lower nitrogen use efficiency, respectively. Changes in the microbial community structures of nitrification and denitrification processes, including increased activity of ammonia-oxidizing bacteria *MND1* and archaea *Candidatus Nitrososphaera* in legume and sweet potato rotations, and a shift in denitrifying microbes of diverse rotations (a decrease in *Rhodoplanes* and an increase in *Paracoccus*), significantly contributed to the overall reductions in emissions in all other investigated rotation systems. Understanding the microbial mechanisms that control N_2O emissions from agricultural soils will enable the development of more effective and crop-specific strategies to further reduce greenhouse gas emissions.

1. Introduction

Nitrous oxide (N_2O) is a greenhouse gas 273 times more potent than carbon dioxide, which persists for about a century, and depletes stratospheric ozone, with profound effects on global climate and atmospheric chemistry (Griffis et al., 2017). Through the application of synthetic nitrogen (N) fertilizers to soils, agriculture contributes to 61 % of anthropogenic N_2O emissions and is becoming the most important sector to address these emissions (IPCC, 2021). This is further exacerbated by the current trends in climate change and escalating global food demand, which relies nowadays in intensified agricultural practices, particularly increased use of N fertilizers (Pan et al., 2022). Therefore, optimization of traditional agricultural practices and a comprehensive understanding of N_2O emission dynamics in agricultural systems are essential for shaping sustainable agroecosystems.

Diversified crop rotations with reduced inputs of N fertilization and herbicides have emerged as a sustainable agricultural strategy that can improve crop productivity, energy use efficiency, soil organic matter,

* Corresponding author.
E-mail address: yangxiaolin429@cau.edu.cn (X. Yang).

https://doi.org/10.1016/j.agrformet.2024.110370
Received 2 June 2024; Received in revised form 18 October 2024; Accepted 13 December 2024
Available online 20 December 2024

nutrient availability, and reducing pest infestation (Beillouin et al., 2021; Krupinsky et al., 2002; Liu et al., 2022; Ma et al., 2023). Despite these advantages, the extent to which crop rotations mitigate N_2O emissions, especially when compared to intensive monocropping, is still debated (Li et al., 2023). Existing studies of crop diversification have reported mixed results, with N_2O emissions increasing, decreasing, or remaining unchanged (Drury et al., 2021; Johnson et al., 2010; Linton et al., 2020). This inconsistency is partly due to the focus of N_2O measurements on specific growth phases within rotations. For instance, Drury et al. (2014) found higher early-season N_2O emissions in fertilized rotational maize than in continuous maize, but overall, continuous maize had higher seasonal emissions due to less efficient crop N uptake. This finding illustrates the complex influence of crop rotation sequences on N_2O emissions and highlights the need to assess these emissions over the entire rotation cycle in the long term, including both cropping and fallow periods (Garnier et al., 2024; Li et al., 2023; Tallec et al., 2022).

While different crop rotations typically require contrasting fertilization rates, it is increasingly recognized that factors beyond N fertilizer application can strongly influence N_2O emissions. Nitrous oxide production in agricultural soils is mainly controlled by the microbial activities of nitrification and denitrification (Harter et al., 2014), which are highly sensitive to soil conditions such as water-filled pore space (WFPS), carbon (C) and N availability, soil temperature, and pH (Reay et al., 2012). Diversified crop rotations can alter soil physical properties, hydrology, and nutrient dynamics, as well as affect soil microbial composition and activity over time, through changes in the quantity and quality of crop residues, root traits, and root exudates (Liang et al., 2023; Linton et al., 2020; Munkholm et al., 2013; Tiemann et al., 2015). These changes may in turn affect soil N_2O emissions (Abalos et al., 2022a; Olesen et al., 2023; Tiemann et al., 2015). Moreover, this effect is probably amplified when different crop species, such as grasses and legumes, are part of the rotation system. Yet, the extent of these effects of rotation diversification beyond fertilization remains unclear, particularly in relation to the microorganisms involved.

Numerous tools have emerged to predict the ecological functions of both prokaryotic and eukaryotic microorganisms using data from amplicon-based next-generation sequencing. These tools not only reveal the types of microorganisms present but also provide insights into what functions they perform within ecosystems (Aßhauer et al., 2015; Louca et al., 2016). Their effectiveness relies on extensive global datasets, making them a cost-effective alternative to full metagenomic sequencing. Among these tools, functional annotation of prokaryotic taxa (FAPROTAX) stands out for its distinctive approach to predict bacterial and archaeal functions and has been used in various systems (Gao et al., 2019; Jiang et al., 2021; Li et al., 2019; Louca et al., 2016). Using FAPROTAX for N_2O studies can provide new insights into how changes in soil microbial communities and functions control these emissions.

The North China Plain, which accounts for 76 % of China's wheat and 29 % of its maize production, predominantly uses a winter wheat and summer maize double-cropping system (WM rotation (Tan et al., 2017). Covering 60 % of the region's cropland, this system often overuses N fertilizer, averaging over 500 kg N ha^{-1} yr^{-1}, well above the optimal 200–300 kg N ha^{-1} yr^{-1} range (Cui et al., 2010; Meng et al., 2012), leading to low N use efficiency and increased N_2O emissions (Cui et al., 2012; Ju et al., 2009). With China's 2060 carbon neutrality goal, it is imperative to transform these high-input, environmentally costly practices into sustainable, environmentally friendly agricultural systems. This will require region-specific land management that balances food production with environmental stewardship. While diversified crop rotations—including grasses, legumes—tested on the same field experiment as our study have shown promise for improving equivalent yields (Yang et al., 2024), their effect on N_2O emissions is understudied. Hence, our focus on long-term monitoring of N_2O emissions in diverse crop rotations is essential to evaluate their environmental efficacy and refine agricultural strategies to meet mitigation goals.

Here, we report on a 6-year field study (2016–2022) of N_2O emissions from traditional and diverse crop rotations. Our study aims to: 1) quantify N_2O emissions and emission factors (EFs) from both traditional WM and diverse crop rotations including legumes, grasses like sweet potato and peanut, and 2) explore the influence of abiotic and biotic factors on N_2O emissions in these systems. Our hypotheses are: 1) Diversified crop rotations, compared to the conventional wheat-maize rotation, reduce N_2O emissions by lowering the relative abundance of nitrifying and denitrifying microbes due to reduced fertilization and irrigation; 2) These diverse rotations yield lower N_2O EFs, attributable to more efficient N use efficiency, compared to the conventional wheat-maize rotation; and 3) Compared to the conventional wheat-maize rotation, the mediation of N_2O emissions by the microbial community structures of nitrification and denitrification processes varies in diversified rotations, influenced by differences in crop residues, root structures, and root exudates (Abalos et al., 2022a; Tiemann et al., 2015).

2. Materials and methods

2.1. Site description

The long-term field experiment was initiated in October 2016 at the Luancheng Agro-Ecosystem Experimental Station, located in Hebei Province, China (37° 50′ N, 114° 40′ E; altitude 50.1 m). Prior to the experiment, the field had a history of cultivating wheat and maize in a year-round double-cropping system. The soil in this study is classified as Ochri-Aquic Cambosols according to the China Soil Taxonomy System, which is equivalent to Aquepts Inceptisols in the US Soil Taxonomy. The top 20 cm layer of the soil has a loam texture with sandy loam characteristics. The region's climate is characterized by a semi-humid warm temperate monsoon climate, with an annual average temperature of 14.7 °C and an average annual precipitation of 472 mm. About 60–70 % of this precipitation occurs from June to September and the area typically experiences around 200 frost-free days each year. Before the experiment, soil analysis of the 0–20 cm layer revealed 12 g kg^{-1} soil organic carbon (SOC), 1 g kg^{-1} of soil total N (TN), 9 mg kg^{-1} of available phosphorus (P), and 110 mg kg^{-1} of available potassium, with a bulk density (BD) of 1.5 g cm^{-3}.

2.2. Experimental design and agronomic management

The field experiment followed a completely randomized block design with three replications. Each plot was 30 m^2 (4 × 7.5 m), and there was a 1 m gap between adjacent plots to avoid interference. The experimental treatments in this study contained the conventional crop rotation (winter wheat (*Triticum aestivum* Lory, 2013) - summer maize (*Zea mays* L., cv. Jundan 20), WM, 1-year cycle) and five diverse crop rotations (all with 3 or 4 harvests in 2 years) (Ryegrass (*Lolium perenne* L., cv. Dongmu 70) - sweet sorghum (*Sorghum bicolor* (L.) Moench., cv. Jintianza 3) → winter wheat - summer maize, RSWM, 2-year cycle; Spring maize (cv. Jundan 20) → winter wheat - summer maize, SmWM, 2-year cycle; Peanut (*Arachis hypogaea* L., cv. Jihua 4) → winter wheat - summer maize, PWM, 2-year cycle; Soybean (*Glycine* max (L.) Merr., cv. Shidou 12) → winter maize – summer maize, SWM, 2- year cycle; Sweet potato (*Ipomoea batatas* (L.) Lam., cv. Shangshu 19) → winter wheat - summer maize, SpWM, 2-year cycle) (Fig. 1). Winter wheat was planted in October and harvested in June, with a sowing rate at 13 kg ha^{-1}. Summer maize, planted in June and harvested in September, had a density of 65,300 plants ha^{-1}. Sweet potatoes and peanuts, sown in April, had densities of 51,300 plants ha^{-1} and 370,400 plants ha^{-1}, respectively, with harvests in October and September. Soybean and spring maize, both planted in April, had densities of 296,300 plants ha^{-1} and 66,700 plants ha^{-1}, and were harvested in September and August. Ryegrass was seeded in October for an April harvest, with a density of 170 kg ha^{-1}. Sorghum, grown from April to September, had a density of 74,700 plants ha^{-1} (Table S1). The same crop in different rotations

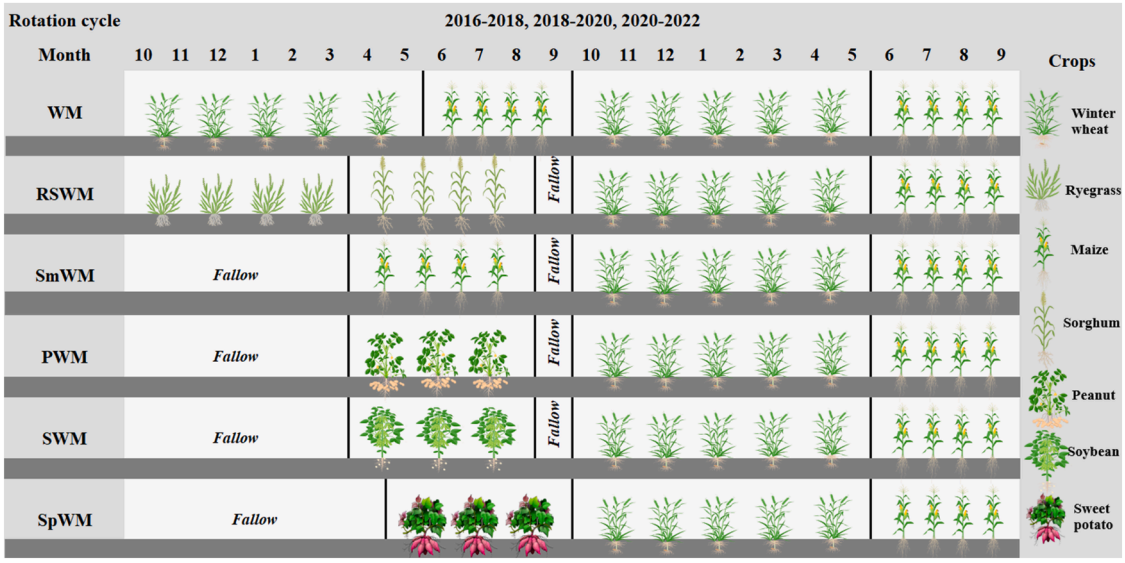

Fig. 1. Schematic diagram of the conventional and diverse crop rotation systems for three rotation cycles from 2016 to 2022. Rotations include WM (Winter wheat - summer maize, 1-year cycle), RSWM (Ryegrass - sweet sorghum → winter wheat - summer maize, 2-year cycle), SmWM (Spring maize → winter wheat - summer maize, 2-year cycle), PWM (Peanut → winter wheat - summer maize, 2-year cycle), SWM (Soybean → winter maize – summer maize, 2- year cycle), and SpWM (Sweet potato → winter wheat - summer maize, 2-year cycle).

received the same irrigation management including time and amount. Scheduling varied based on crop growth stages: winter wheat was irrigated at overwintering, jointing, and anthesis; summer maize at sowing and large trumpet stages; sweet potato at sowing and tuber expansion; peanut and soybean at sowing and podding; ryegrass during overwintering, middle, and later stages; and sorghum and spring maize at sowing and flowering. Each time received around 75 mm irrigation water. The detailed information was supplied in Table S2. The WM and RSWM systems averaged 375 mm and 338 mm annually, respectively, compared to 263 mm for other systems. Fertilization consisted of applications of N (urea), phosphorus (P_2O_5), and potassium (K_2O). Application rates were determined based on the practical experience of local farmers to reflect common agricultural practices in the region. The annual N application rate for the WM system was 594 kg ha^{-1} (118.5 kg ha^{-1} base and 191.7 kg ha^{-1} top dressing for winter wheat, 283.7 kg ha^{-1} top dressing for summer maize). In the other rotation systems, the N application rates for winter wheat and summer maize were the same as in the WM system. Specifically, the additional crops in the rotations received the following N amounts: RSWM applied 118.5 kg ha^{-1} base N for ryegrass and 134.8 kg ha^{-1} base plus 89.7 kg ha^{-1} top dressing to sorghum; SmWM applied 134.8 kg ha^{-1} base plus 89.7 kg ha^{-1} top dressing to spring maize; PWM applied 75 kg ha^{-1} base plus 81.3 kg ha^{-1} top dressing to peanut; SWM applied 151.8 kg ha^{-1} base to soybean; and SpWM applied 27 kg ha^{-1} base to sweet potato (Table S2). Residue management varied between crops and was closely related to their harvesting practices. After harvesting winter wheat, about 20 cm of stubble was left, and the remaining straw was chopped and mulched on the soil. For summer maize, all straw was chopped and incorporated to a depth of 20 cm using a rotary tiller. For sweet potatoes and peanuts, the entire aboveground biomass, including roots, was removed by hand. Soybeans were harvested, leaving only the roots behind. Sorghum was harvested manually, leaving 5–10 cm of stubble and roots, while ryegrass was completely removed, leaving only the roots. Thus, except for wheat and maize, most crop residues were removed. Before the next planting event, all the soil was tilled to a depth of 20 cm with a rotary tiller.

2.3. Field N_2O fluxes

Measurements of N_2O fluxes were performed using the static chamber method (Clayton et al. 1994; Zheng et al., 2008). We placed a plastic base frame into the soil 5 cm between crop rows in the center of each plot and placed one chamber (20 cm × 20 cm × 30 cm) on top of the frame for gas collection. Water sealed the channels between the chamber and the frame during measurements. Each chamber had a fan to maintain uniform gas concentration and a thermometer to track temperature during gas collection. Gas samples with > 30 mL per sample were taken from 9:00 in the morning using a 100 ml syringe connected to a triple stopcock at specific time intervals (0, 12, 24, and 36 min) after closing the chamber, which reflects the daily N_2O flux rate (Noemi Cosentino et al., 2012). Sampling was weekly from planting to harvest but increased to every three days after fertilizing, irrigation, or heavy precipitation events. The N_2O concentrations were then analyzed using a gas chromatograph (Agilent 7890 A, Agilent Inc., USA) with a micro electron capture detector at 330 °C. The carrier was high-purity N_2 (99.999 %) at a flow rate of 20 mL min^{-1}, and a purge gas mixture containing 5 % CO_2 in N_2 was used to prevent interference from CO_2 during the measurements. The minimum detectable flux was 30 ppb.

2.4. Weather data, soil temperature and water content

The meteorological station, located 100 m from the Luancheng experimental site, provided daily precipitation and air temperature data. T-type thermocouples were installed near the gas chamber for each plot to continuously measure soil temperature at 5 cm depth, with readings taken hourly and stored using a data logger (HOBO, Onset, USA). Soil water content was measured manually at 20 cm depth during each gas sampling event using a standard thermo-gravimetric method to guarantee accuracy, to avoid the near-surface inconsistencies that can occur with sensors such as neutron probe or time domain reflectometry.

2.5. Soil sampling and analysis

Soil sampling from each plot following summer maize harvest happened in October 2022, with a total of 18 soil samples taken. Surface plant litter was first cleared manually. From each plot, five soil subsamples were extracted from the top 20 cm using an auger. These were then mixed to form a homogenized sample for each plot. Each composite sample was immediately preserved in dry ice, transported to the laboratory, and sieved through a 2 mm mesh to remove stones and

root debris. A portion of each fresh composite sample was allocated for soil microbial analysis, while the remaining soil was processed to examine its physicochemical properties.

Soil bulk density at a 0–20 cm depth was measured in each plot after each crop harvest during the experiment period using the gravimetric method (Grossman and Reinsch, 2002). Soil pH was determined in a soil suspension with a water to soil ratio of 5:1 (Mclean, 1983). Soil organic carbon was measured using the combustion method with a vario Macro CNS Analyzer (Elementar, Germany). Prior to test, soil samples were first oven dried at 105 °C for 24 h, then treated with 0.5 M hydrochloric acid to eliminate carbonates, followed by ball milling for homogenization (Harris et al., 2001). Total nitrogen (TN) was measured via a modified Kjeldahl method (Bremner and Shaw, 1958). Mineral N was measured according to a modified Bremner's protocol (Bremner, 1965). Briefly, 10 g soil was extracted with 2 M KCL, vortexed for 30 min and filtered for analysis using a spectrophotometer (UV-1800 Mapada Instruments, Shanghai, China). Soil available P was extracted using 0.5 mol L^{-1} $NaHCO_3$ (pH 8.5) followed by the molybdenum blue colorimetric method (Olsen and Sommers, 1982). Microbial biomass carbon (MBC) and nitrogen (MBN) were measured by the chloroform fumigation extraction method (Vance et al., 1987). Briefly, soil samples (10 g) were exposed to alcohol-free chloroform ($CHCl_3$) vapor within a vacuum desiccator containing NaOH solution for 24 h at room temperature. Residual $CHCl_3$ was removed by repeated evacuations after fumigation. Soils (fumigated and non-fumigated) were immediately extracted by shaking for 30 min with 40 mL of 0.5 M K_2SO_4. The filtered extracts were measured with the TOC analyzer (Multi 3100N/C, Analytik Jena, Germany). Dissolved organic carbon (DOC) was measured by extracting 5 g of fresh soil with 50 mL of 0.25 M K_2SO_4 for 30 min at 200 rpm. The supernatant was filtered through a 0.45 μm filter, and the DOC concentration was analyzed using a TOC analyzer (MultiN/C 3100, Analytik Jena AG, Jena, Germany).

2.6. Soil DNA extraction, sequencing, and microbial functions related to N cycling by faprotax analysis

We extracted soil DNA utilizing the Powersoil DNA Isolation Kit (Mo Bio Laboratories, Carlsbad, CA, USA), following the manufacturer's protocol. Briefly, lyophilized soil (0.5 g) was lysed with a buffer, centrifuged, and the supernatant was applied to a silica filter for DNA binding. After washing off impurities, DNA was eluted with a buffer. The integrity of the DNA was evaluated using a NanoDrop spectrophotometer (ND2000, Thermo Scientific, Wilmington, DE), with the absorbance ratios at 260/280 nm and 260/230 nm being assessed. The extracted DNA was then preserved at −80 °C for subsequent analyses. In order to amplify the bacterial 16S rRNA gene, a primer pair barcode-515F/806R (5′-GTGCCAGCMGCCGCGGTAA-3′/5′-GCACTACHVGGGTWTCTAAT-3′) targeting the V3+V4 region was employed, following Caporaso et al. (2010). This approach is known for its accuracy in bacterial taxonomy and minimal bias across different bacterial groups. The polymerase chain reaction (PCR) reactions were conducted in a 50 μl mix comprising 2 μl of the DNA template (ranging from 1 to 10 ng), 5 μl of each primer at 2 μM, 25 μl Premix Ex Taq (Takara Biotechnology), and 13 μl of sterilized water. The thermal cycling protocol included an initial 3-minute denaturation at 94 °C, six touchdown cycles (45 s at 94 °C, 60 s decreasing from 65 °C to 58 °C, 70 s at 72 °C), followed by 22 cycles (45 s at 94 °C, 60 s at 58 °C, 60 s at 72 °C), and a final 10-min extension at 72 °C. High-throughput sequencing for the tag-encoded 16S genes, including purification and quantification of PCR products, was executed by Magigene Company (Beijing, China) using the Illumina MiSeq platform. Quality processing of raw sequences was conducted using the Quantitative Insights Into Microbial Ecology (QIIME) pipeline (version 2.1) (Bokulich et al., 2013; Caporaso et al., 2010). We performed resampling of operational taxonomic units (OTUs) based on the lowest sequence count to normalize sampling. OTUs were clustered at 97 % similarity using the UPARSE pipeline (version 7.1, Edgar, 2013) and annotated through the GreenGene Database, utilizing the ribosomal Database Project (RDP) Classifier (Version 2.2) after discarding singletons (Edgar, 2013).

Prokaryotic OTUs were classified using FAPROTAX (v.1.2.4) (Louca et al., 2016). This tool assigns ecological functions by matching taxa from the annotated OTU tables to functional phenotypes of each taxon in the FAPROTAX database. Initially developed for marine environments, the FAPROTAX database contains over 80 functions and detailed taxonomic data for over 4600 bacterial and archaeal species (Louca et al., 2016). The FAPROTAX is versatile and applicable to both aquatic and terrestrial ecosystems (Jiang et al., 2021; Shi et al., 2020; Zhang et al., 2022), as it incorporates taxonomic references such as Bergey's Manual of Systematic Bacteriology (Goodfellow, 2012; Vos et al., 2011), the Prokaryotes (Lory, 2013), and the International Journal of Systematic and Evolutionary Microbiology (International Journal of Systematic and Evolutionary Microbiology 2024) to classify bacteria and archaea from both aquatic and terrestrial ecosystems. Functional assignments are not strictly habitat dependent, but are largely based on taxonomic details at the genus, species, or strain level. In other words, FAPROTAX emphasizes taxonomy over the environment when assigning ecological functions. In our study, OTUs were first normalized and then mapped to the FAPROTAX database using Python, which automatically annotated them with functional information. Most species were involved in key processes, such as the biogeochemical cycles of C, N, sulfur, and organic matter decomposition. We focused on N cycling processes (Description S1 in the Supplementary Materials), especially nitrification and denitrification, which are the main biological sources of N_2O emissions. A table was created to show the relative abundance of microbiota of functional processes across different crop rotation systems. To specifically identify the microbial taxa involved in these processes, we extracted the OTUs annotated for relevant functions and analyzed them at the family, genus, or species level. By calculating the relative abundance of these taxa within each sample, we compared their distribution across different rotation systems and assessed their roles in N_2O emissions.

2.7. Calculations and statistical analysis

Soil WFPS (0–20 cm, %) was calculated during each gas sampling event using the method of Hillel (1980):

$$WFPS\ (\%) = \frac{SWC}{1 - \frac{BD}{PD}} \tag{1}$$

where PD is particle density for inorganic soils (2.65 g cm^{-3}), SWC is soil water content (0–20 cm, %), and BD is the soil bulk density (0–20 cm, g cm^{-3}).

Soil N_2O flux (f, $\mu g\ m^{-2}\ h^{-1}$) were calculated as following:

$$f = \frac{m}{V_m} \times \frac{T_0}{T} \times \frac{P}{P_0} \times H \times \frac{\Delta C}{\Delta t} \times 60 \tag{2}$$

where m is the molecular weight of N_2O (44 g mol^{-1}), and V_m is the standard molar volume of an ideal gas ($m^3\ mol^{-1}$), T_0 (K) is the ideal gas temperature, T (K) and P (kPa) are the air temperature and pressure in the chamber at the sampling time, P_0 (kPa) being the standard atmospheric pressure H (m) is the height of chamber. $\Delta C/\Delta t$ (ppm) is slope of the linear regression curve for the change of the N_2O concentration during times of chamber closure ($\mu g\ m^{-3}\ h^{-1}$), 60 is min h^{-1}.

Cumulative N_2O emissions (F, kg ha^{-1}) during crop growing season and fallow period were calculated using linear interpolation between successive sampling days, as described by (Xiao et al., 2022):

$$F = \sum_{i=1}^{n} \left[\frac{f_i + f_{i+1}}{2} \times (t_{i+1} - t_i) \right] \times 24 \times 10^{-5} \tag{3}$$

where f is the N_2O flux rate ($\mu g\ m^{-2}\ h^{-1}$), i is the i^{th} measurement, (t_{i+1} −

t_i) is the number of days between two consecutive measurements. 24 (h day^{-1}) is the conversion from a min^{-1} to a day^{-1} and 10^{-5} converts μg m^{-2} to kg ha^{-1}.

Emission factors (EFs) (%) for each rotational cycle were determined as the percentage ratio of cumulative N_2O emissions (kg ha^{-1} yr^{-1}) to total fertilizer inputs (kg ha^{-1} yr^{-1}), without accounting for N_2O emissions from an unfertilized control (Abalos et al., 2016). Emission factors evaluate the environmental impact of agricultural methods. A higher cropping system EF indicates increased conversion of fertilizer N to N_2O, signifying over-fertilization or inefficient fertilizer application (Abalos et al., 2016).

$$EFs\ (\%) = \frac{\text{cumulative } N_2O \text{ emissions}_{i,t}}{\text{total fertilization}_{i,t}} \quad (4)$$

where "*i*" represents different crop rotations and "*t*" represents different rotation cycles (2016–2018, 2018–2020, 2020–2022).

All the statistical analyses and visualizations were performed in R version 4.0.5 (R Development Core Team, 2020). Prior to statistical analyses, all data were checked for normality and homogeneity of variances using the Shapiro-Wilk test (ks.test) and Levene's test (leveneTest), respectively. Log-transformed where necessary before analysis (i.e. cumulative N_2O). The impact of different rotation systems on N_2O emissions, EFs, soil (soil pH, SOC, TN, DOC, mineral N, and SWC) and microbial variables (MBC, MBN and microbial functions related to N cycling) was examined using one-way ANOVA, with mean comparisons via Tukey's test at $P < 0.05$ using the "emmeans" package. Z-score standardization was applied to the relative abundances of N-cycling functional processes to account for differences across the various rotation systems. Principal Component Analysis (PCA) was utilized to discern similarities and differences among cropping systems and understand the relationships between observed variables using the "FactoMineR" package. Redundancy Analysis (RDA), executed with the "vegan" package, was applied to explore the associations between response variables (N_2O and SOC) and explanatory variables (environmental and microbial factors). The significance of these explanatory variables was assessed using Monte Carlo permutation tests with 999 permutations. Linear regression analysis was used to investigate the correlation between cumulative N_2O emissions and potential influencing factors.

3. Results

3.1. Dynamics of precipitation, air temperature, soil temperature, WFPS and N_2O flux

Over the six years of field experiment, the mean daily temperature was 14.3 °C, and the mean annual precipitation was 430 mm. The total annual precipitation of the three rotation cycles from 2016 to 2018, 2018 to 2020, and 2020 to 2022, was 369, 381, and 539 mm yr^{-1}, respectively (Fig. 2, Table S3). During the entire measurement cycle, the average soil temperatures at 0–5 cm for WM, RSWM, SmWM, PWM, SWM, and SpWM rotations were 18.7, 19.5, 19.5, 19.4, 19.1, and 19.3 °C, respectively ($P < 0.001$). The average WFPS at 0–20 cm of these rotations were 67.8, 68.5, 68.5, 64.0, 64.7, and 65.8 %, respectively ($P < 0.001$, Fig 3, Table S3).

In crop rotation systems, N_2O fluxes remained low in the absence of fertilization, precipitation or irrigation but were more variable during the summer. Fertilization, either alone or combined with irrigation or precipitation, resulted in peaks of N_2O emissions 1–3 days after application (Fig. 3, S1, S2, S3). This effect was especially notable during the summer maize season, where top-dressing fertilizer combined with irrigation increased N_2O fluxes in all systems, with the WM system showing the largest increase ($P < 0.01$). In contrast, irrigation alone had inconsistent effects, sometimes increasing N_2O fluxes and other times showing no change during winter wheat period. After wheat and maize harvests, incorporating chopped residues via mulch or rotary tillage (0–30 cm) increased N_2O emissions, particularly when combined with N fertilization and approximately 90 % WFPS. In the WM system, summer maize residue incorporation followed by winter wheat seeding and fertilization led to a maximum 700 % increase in N_2O emissions compared to previous measurements ($P < 0.001$). The degree of N_2O

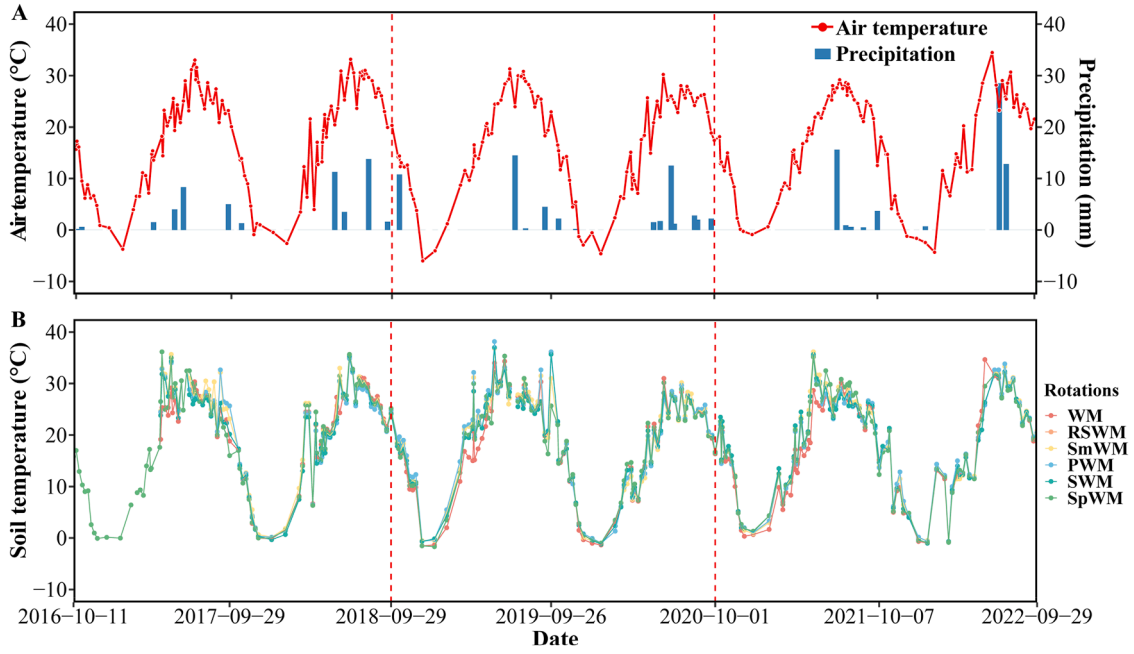

Fig. 2. Temporal variations in daily air temperature, daily precipitation, and soil temperature during gas sampling events across different rotations from 2016 to 2022. The red dotted lines are separating the different rotation cycles. Rotations include WM (Winter wheat - summer maize, 1-year cycle), RSWM (Ryegrass - sweet sorghum → winter wheat - summer maize, 2-year cycle), SmWM (Spring maize → winter wheat - summer maize, 2-year cycle), PWM (Peanut → winter wheat - summer maize, 2-year cycle), SWM (Soybean → winter maize – summer maize, 2-year cycle), and SpWM (Sweet potato → winter wheat - summer maize, 2-year cycle).

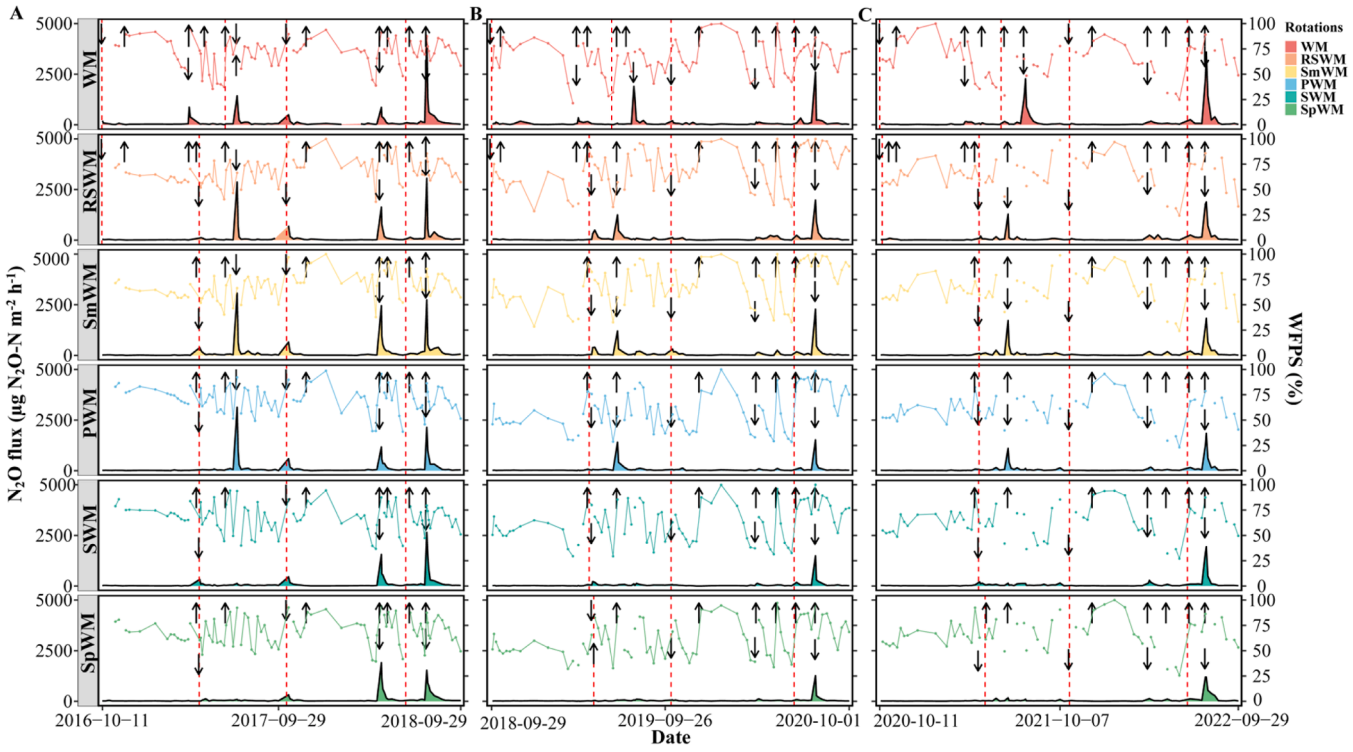

Fig. 3. Temporal dynamics of water-filled pore space at 0–20 cm (WFPS) and nitrous oxide (N_2O) flux in different crop rotations over a six-year period from 2016 to 2022. The data are presented in three panels corresponding to the three rotation cycles: Panel A (2016–2018), Panel B (2018–2020), and Panel C (2020–2022). Colored area plots represent the average N_2O flux, while line plots represent the average WFPS. Upward arrows indicate irrigation, and downward arrows indicate fertilization. The red dotted lines are separating the sowing times of the different crops in the rotations. Rotations include WM (Winter wheat - summer maize, 1-year cycle), RSWM (Ryegrass - sweet sorghum → winter wheat - summer maize, 2-year cycle), SmWM (Spring maize → winter wheat - summer maize, 2-year cycle), PWM (Peanut → winter wheat - summer maize, 2-year cycle), SWM (Soybean → winter maize – summer maize, 2- year cycle), and SpWM (Sweet potato → winter wheat - summer maize, 2-year cycle).

increased after fertilization and/or irrigation and precipitation varied between systems (Fig. 2, 3, S1, S2, S3). When analyzing the average N_2O flux over two-year rotation cycles, PWM, SWM, and SpWM had lower N_2O fluxes than WM, RSWM, and SmWM, regardless of the rotation cycle. WM had the highest average N_2O flux among all cropping systems, with mean values of 193, 133, and 187 μg N_2O—N m^{-2} h^{-1} over the three cycles, respectively (Table S3).

3.2. Cumulative N_2O emissions and emissions factors

Annual cumulative N_2O emissions varied across the crop rotations over the three cycles (Fig. 4A), initially ranging from 6 to 10 kg ha^{-1} yr^{-1} in 2016–2018, decreasing to 4–8 kg ha^{-1} yr^{-1} in 2018–2020, and fluctuating between 4 and 9 kg ha^{-1} yr^{-1} in 2020–2022. Although precipitation significantly increased in 2020–2022, N_2O emissions remained lower than in the first cycle ($P < 0.01$). Across all cycles, the WM rotation consistently resulted in the highest N_2O emissions ($P < 0.001$, $P < 0.001$, $P < 0.001$). In contrast, SWM and SpWM rotations maintained lower emission levels. Over the six-year period, diversified rotation systems reduced N_2O emissions by 23 %−49 % compared to conventional WM rotation (Fig. 4A, $P < 0.001$). Specifically, WM exhibited the highest average cumulative emissions at 9 kg ha^{-1} yr^{-1}. The SpWM rotation achieved the most significant reduction, with a decrease of 4 kg ha^{-1} yr^{-1} ($P < 0.001$), followed by SWM, PWM, and RSWM, which reduced emissions by 4, 3, and 2 kg ha^{-1} yr^{-1}, respectively ($P < 0.001$, $P < 0.001$, $P < 0.001$), in comparison to WM (Fig. 4A). The ranking of crop rotations in terms of EFs differed from the order of cumulative N_2O emissions. Over the six-years across rotation systems, SWM and SpWM rotations had the lowest average EF_S, while SmWM rotations had the highest, followed by PWM rotation systems (Fig. 4B, $P < 0.001$).

3.3. Soil properties and microbial functions associated with N cycling

Soil pH, soil temperature, WFPS, and MBN measured after the experiment did not differ significantly among rotation systems ($P = 0.66$, $P = 0.73$, $P = 0.2$, $P = 0.94$). SOC was highest in the SpWM system across all crop rotations (14 g kg^{-1}), an 8 % increase compared to the WM system ($P = 0.05$). TN was highest in the WM system (1 g kg^{-1}, $P = 0.03$). The soil C/N ratio was also higher in SWM and SpWM systems compared to WM ($P = 0.03$, $P = 0.007$). Ammonium levels were significantly higher in the WM and SpWM rotations ($P < 0.001$), with the highest NO_3^- concentrations observed in the SWM system ($P = 0.04$). The concentration of MBC was highest in RSWM (321 mg kg^{-1}), 65 % higher than WM (Fig. S5, $P = 0.001$). The highest DOC concentration was found in the PWM system (61 mg kg^{-1}, $P < 0.001$).

Our Z-score analysis further highlighted the differences in the relative abundance of microbial N-cycling functions across systems (Fig. 5). A contrasting effect was observed between the two legume-based cropping systems, with a higher trend in SWM compared to PWM (Fig. 5A). Across all crop rotation systems, the RSWM system showed the highest relative abundance of nitrifying microbes at 19.6 %, while the SpWM system recorded the lowest at just 9 % ($P < 0.001$). The WM and RSWM systems had the highest relative abundance of denitrifying microbes among all the systems (Fig. 5A, $P = 0.01$). Our Sankey diagram delineated the linkages between these crop rotations, specific N processes (nitrification and denitrification), and dominant microbial taxa across the kingdom, family, and genus levels (Fig. 5B). During nitrification, the predominant microbial microbes involved the Nitrosomonadaceae family (including the genus *Ellin6067, IS-44, MND1,*

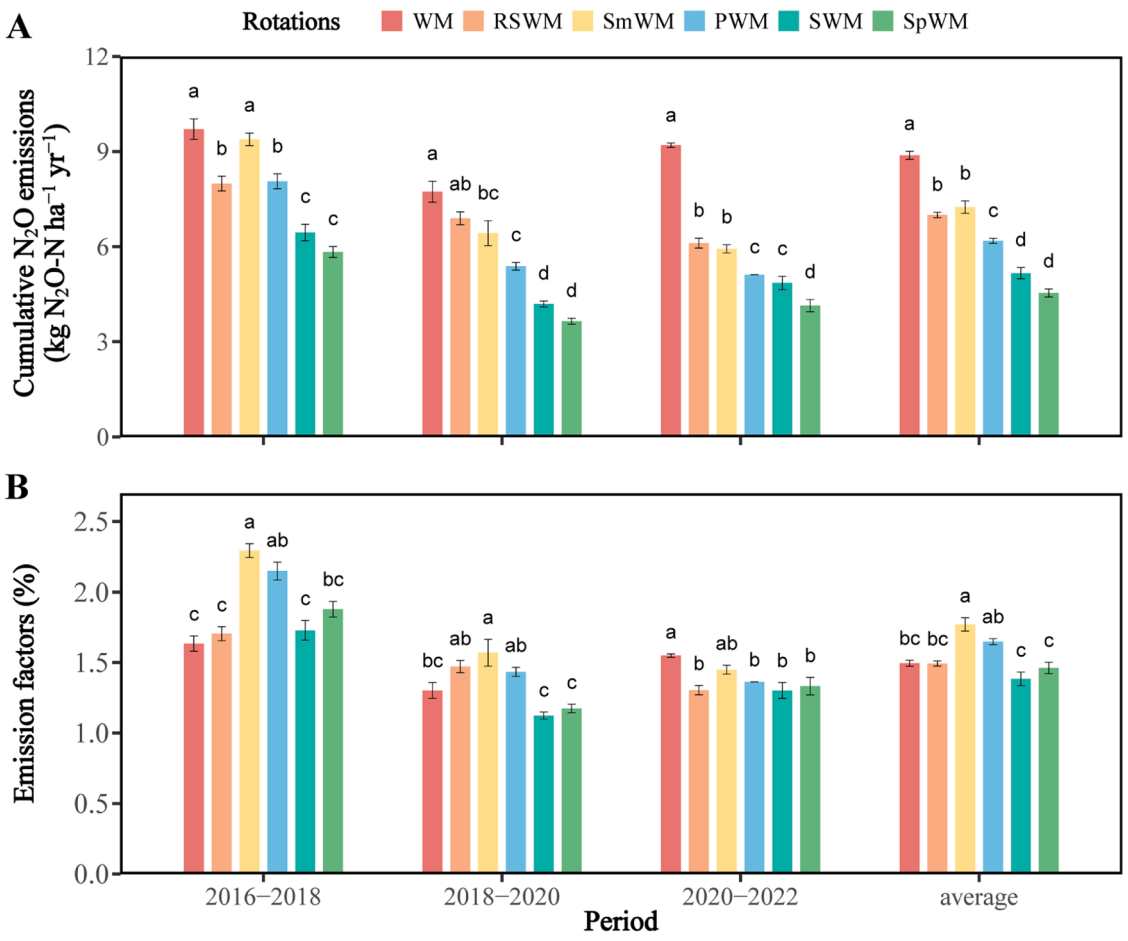

Fig. 4. Mean cumulative N_2O emissions (A) and emission factors (B) across different rotations and periods. Rotations include WM (Winter wheat - summer maize, 1-year cycle), RSWM (Ryegrass - sweet sorghum → winter wheat - summer maize, 2-year cycle), SmWM (Spring maize → winter wheat - summer maize, 2-year cycle), PWM (Peanut → winter wheat - summer maize, 2-year cycle), SWM (Soybean → winter maize – summer maize, 2- year cycle), and SpWM (Sweet potato → winter wheat - summer maize, 2-year cycle). Bars represent mean ± SE. Lower case letters indicate significant differences at the level of 0.05.

Nitrosospira) and the Nitrospiraceae family (genus *Nitrospira*), along with the archaeal family Nitrososphaeraceae (including *Candidatus Nitrososphaera* and an unidentified genus). The relative abundance of microbial communities involved in both nitrification and denitrification significantly varied among the crop rotations ($P < 0.05$, $P < 0.001$). Specifically, compared to the WM system, the RSWM system exhibited a higher presence of *Candidatus Nitrososphaera* but lower levels of *Ellin6067* and *MND1*. In the PWM, SWM, and SpWM rotations, *MND1* levels were higher compared to WM, while an unidentified genus in the Nitrososphaeraceae decreased. Additionally, *Candidatus Nitrososphaera* increased in PWM and SWM. For denitrification, the key bacterial families were Xanthobacteraceae (genus *Rhodoplanes*) and Rhodobacteraceae (genus *Paracoccus*). WM and SmWM systems had higher levels of *Rhodoplanes* and lower levels of *Paracoccus*.

3.4. Abiotic and biotic drivers of N_2O emissions

The PCA and RDA show the relationships between soil properties, the relative abundances of nitrifying and denitrifying microbes, and N_2O emissions (Fig. 6AB). TN was positively correlated with N_2O emissions, while SOC and the soil carbon to nitrogen (C/N) ratio were negatively correlated with N_2O emissions (Fig. 6A, S5). The RDA also showed the significant influence of management practices, environmental factors, and microbial processes of N cycling on N_2O emissions ($P < 0.001$). Fertilization and irrigation practices, along with the relative abundances of nitrifying and denitrifying microbes, MBC, and TN, were positively correlated with the first axis, which alone explained a substantial (80 %) portion of the variance (Fig. 6B). The relative abundances of nitrifying and denitrifying microbes in crop rotations were also positively related to N_2O emissions ($P = 0.04$, $P = 0.003$, Fig. 6CD).

4. Discussion

4.1. Nitrous oxide dynamics in crop rotation systems

We observed distinct patterns of N_2O emissions fluxes in response to agricultural practices (Fig. 3). When fertilization was the only intervention, a peak in N_2O emissions typically occurred two days after application. This effect was amplified when fertilization coincided with irrigation or precipitation, leading to significant increases in emissions. In the North China Plain, the groundwater table is typically >10 m below the surface, and the soil's WFPS is generally <70 % (Yuan and Shen, 2013). Thus, the combination of high soil moisture following precipitation or irrigation and abundant mineral N from fertilization, provided optimal conditions for denitrifiers (Abalos et al., 2016; Oates et al., 2016; Fig. S4). However, the sharp increase in N_2O emissions during the summer maize season, especially in the WM system, is likely due to excessive N fertilizer application – well above the optimal range of 200–300 kg N ha^{-1} yr^{-1} (Cui et al., 2010; Meng et al., 2012) – exceeding crop uptake capacity. The excess N fuels microbial nitrification and denitrification, driving N_2O emissions. Irrigation also influenced N_2O flux at different winter wheat growth stages (overwintering, jointing, and anthesis). Over-irrigation during jointing can oversaturate the soil with WFPS >90 %, reducing oxygen levels and enhancing

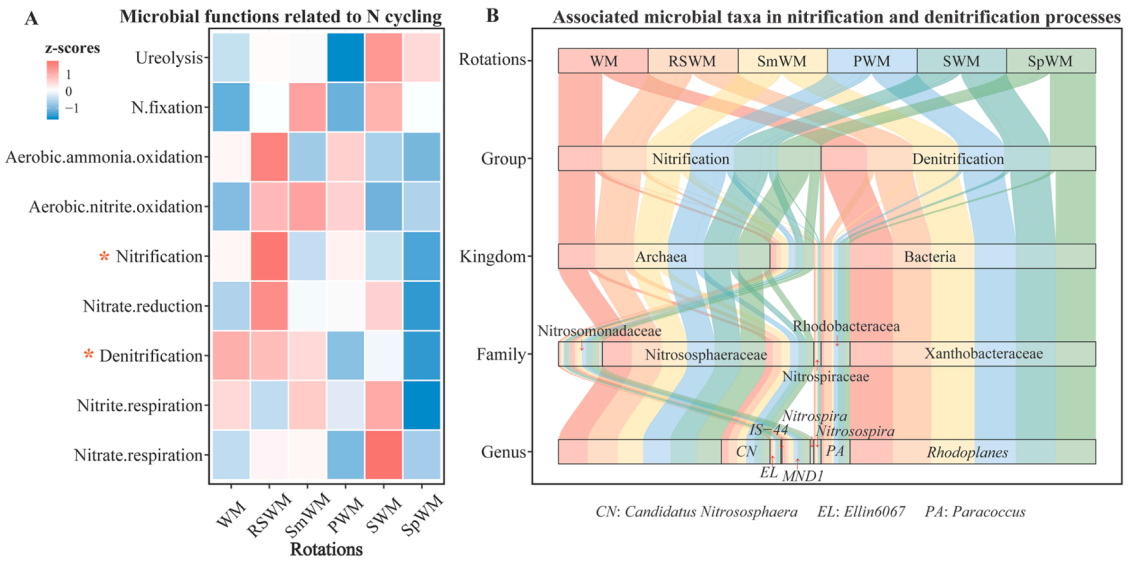

Fig. 5. Comparative analysis of microbial functions related to nitrogen (N) cycling and associated microbial taxa involved in nitrification and denitrification processes across different crop rotation systems, based on Functional Annotation of Procaryotic Taxa (FAPROTAX) analysis. Panel A shows Z-score normalization based on the mean relative abundance (not actual intensity) of microbial functions related to N cycling calculated for each cropping system ($n = 3$), scaled by row. The color scale illustrates differences in the relative abundance of microbial functions involved in N cycling processes across systems, with red indicating higher (z-score = 1), white for neutral (z-score = 0), and blue indicating lower values (z-score = −1). The processes assessed include ureolysis, N fixation, aerobic ammonia oxidation, aerobic nitrite oxidation, nitrification, nitrate reduction, denitrification, nitrite respiration and nitrate respiration. The symbols "*" indicate functions with significant differences at $P < 0.05$. Panel B presents a Sankey diagram that shows the linkages between crop rotation systems, nitrification and denitrification process, and the predominant microbial taxa at various taxonomic ranks. The widths of the flows in the Sankey diagram correspond to the relative abundance of microbial taxa at genus level to each rotation system. Rotations include WM (Winter wheat - summer maize, 1-year cycle), RSWM (Ryegrass - sweet sorghum → winter wheat - summer maize, 2-year cycle), SmWM (Spring maize → winter wheat - summer maize, 2-year cycle), PWM (Peanut → winter wheat - summer maize, 2-year cycle), SWM (Soybean → winter maize – summer maize, 2-year cycle), and SpWM (Sweet potato → winter wheat - summer maize, 2-year cycle).

denitrification, which leads to increased N_2O emissions. This is likely due to lower water uptake compared to the anthesis stage, where water needs are higher. While overwintering also requires less water, colder temperatures during this stage reduce microbial activity and N_2O emissions. Thus, N fertilization and irrigation should be aligned with the specific N and water requirements at each growth stage to reduce N_2O emissions in wheat and maize rotations.

Agricultural N_2O emissions are influenced not only by N fertilization and irrigation but also by the combined effects of tillage and post-harvest residue management. These practices collectively impact the availability of organic substrates, oxygen levels, and WFPS. According to the IPCC (2019), about 1 % of the N in crop residues is converted to N_2O emissions, although in reality this number vary significantly depending on local conditions such as climate, soil type, and crop species (Olesen et al., 2023). Our long-term flux measurements suggested higher N_2O emissions in systems like wheat-maize (WM) rotations, where crushed residues were incorporated into the soil to a depth of 30 cm via rotary tillage, compared to rotations like sweet potato or peanut, where residues were fully removed (Fig. 3). Research by Abalos et al. (2022) indicates that incorporating crop residues increases soil N_2O emissions by 40–50 % compared to systems where residues are removed. This is due to the temporary but substantial supply of C and N-rich organic matter from crushed wheat and maize residues, which enhances microbial activity, promoting both nitrification and denitrification (Chen et al., 2013). Moreover, residue incorporation reduces oxygen diffusion, particularly at greater soil depths, creating anaerobic microsites that promote denitrification, a key pathway for N_2O production (Abalos et al., 2022b; Petersen et al., 2011). In the WM system, this effect is further intensified by synthetic N fertilizer applications for next planting coinciding with residue incorporation when WFPS was about 90 %, fostering a synergy between residue management, fertilization, and moisture that accelerates N_2O emissions (Taghizadeh-Toosi et al., 2021).

In terms of seasonal and yearly patterns, N_2O emissions were especially pronounced during summer, with most precipitation occurring between June and September (Fig. 2). The simultaneous occurrence of rain and higher temperatures during this season makes summer a critical period for soil N_2O flux in this region due to the optimal conditions for high microbial activity (Wang et al., 2013). Interestingly, we observed a decrease in N_2O emissions during the third rotation cycle, despite significantly higher precipitation compared to the first cycle (Fig. 4A, Table S3). This contrasts with the expectation that higher precipitation would enhance N_2O emissions through increased soil moisture. A possible explanation is the uneven precipitation distribution during the third cycle. For example, a short but intense precipitation event of 43 mm in the third cycle likely caused rapid soil saturation, increasing WFPS levels to up to 93 % (Fig. 3). This created anaerobic conditions that inhibited oxygen diffusion and enhanced complete denitrification. Under these conditions, N_2O may have been further reduced to N_2, resulting in lower cumulative N_2O emissions associated with increased overall denitrification activity (Rohe et al., 2021; Schlüter et al., 2024). In addition, the excess precipitation in a short period of time may have caused significant nitrate leaching from the sandy loam soil (Zong et al., 2024). Since nitrate is a key substrate for N_2O production, its depletion through leaching would limit the nitrate available for denitrification, further contributing to the observed reduction in N_2O emissions.

4.2. *Potential abiotic mechanisms driving N_2O emission reductions*

Fertilization and irrigation are critical determinants of cumulative N_2O emissions across different crop rotations (Fig. 6; Table S2). Diversified rotations have inherently lower fertilization and irrigation requirements than conventional winter wheat and summer maize rotations for several reasons. Legumes in our rotations, such as soybeans and peanuts, reducing dependence on synthetic fertilizers by as much as 37 % (Table S3) because of natural biological N fixation. Reductions in

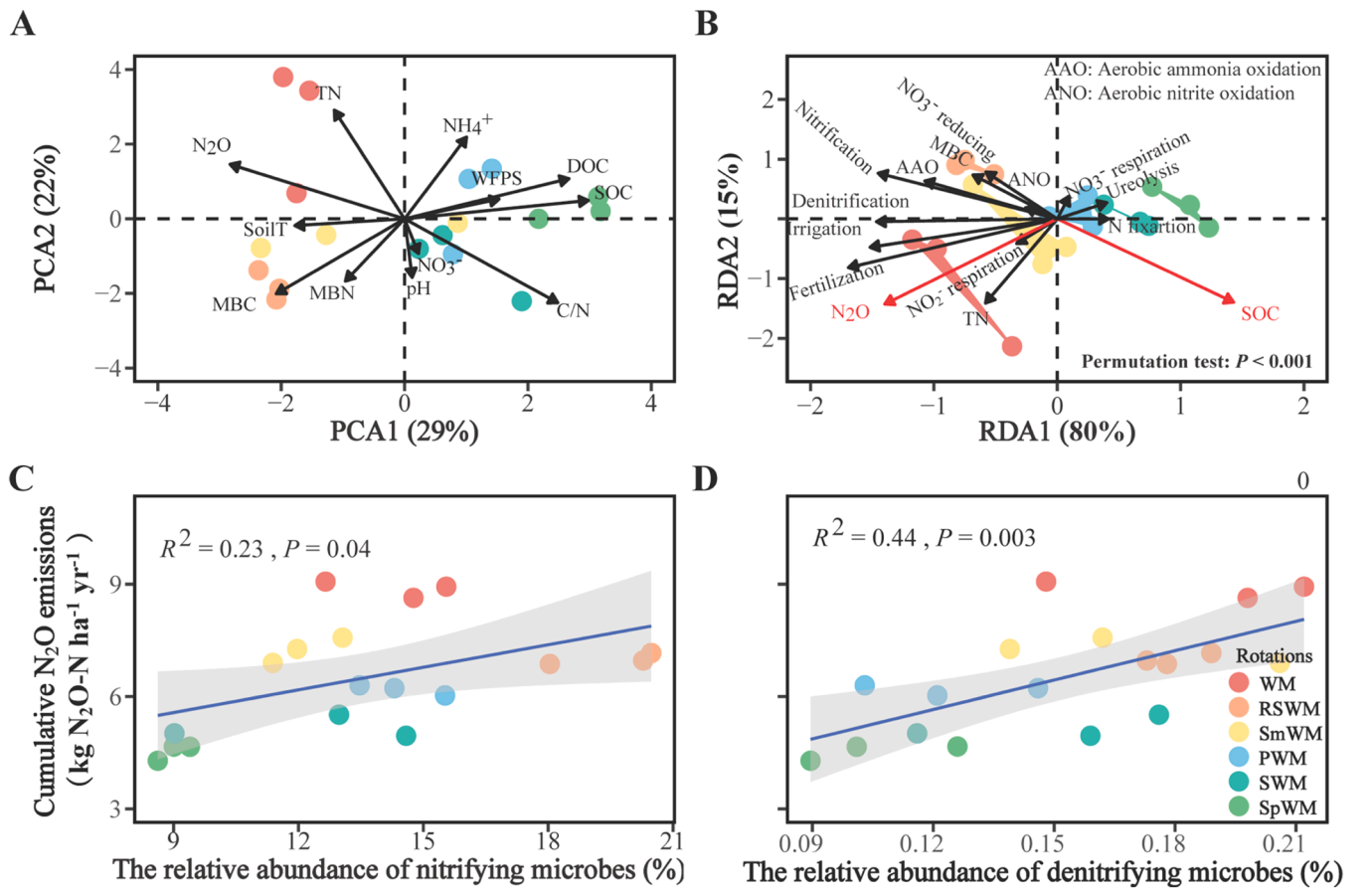

Fig. 6. Abiotic and biotic drivers of N_2O emissions in different crop rotation systems. Panel A (principal component analysis) reveals how soil properties contribute to variations in N_2O emissions. Panel B (redundancy analysis (RDA)) further refines these associations between microbial processes and management practices and N_2O emissions and SOC, with the RDA1 axis and RDA2 axis accounting for 80 % and 15 % of the variation, respectively. Panel C and D shows the relationship between the relative abundances of nitrifying, denitrifying microbes and cumulative N_2O emissions ($R^2 = 0.23$, $P = 0.04$; $R^2 = 0.44$, $P = 0.003$). The gray area in panels C and D represents the 95 % confidence interval (CI) around the regression line. WFPS, water filled pore space; TN, total soil nitrogen; SoilT, soil temperature; SOC, soil organic carbon; NH_4^+, ammonia; NO_3^-, nitrate; MBN, microbial biomass nitrogen; MBC, microbial biomass carbon; DOC, dissolved organic carbon. WM (Winter wheat - summer maize, 1-year cycle), RSWM (Ryegrass - sweet sorghum → winter wheat - summer maize, 2-year cycle), SmWM (Spring maize → winter wheat - summer maize, 2-year cycle), PWM (Peanut → winter wheat - summer maize, 2-year cycle), SWM (Soybean → winter maize – summer maize, 2-year cycle), and SpWM (Sweet potato → winter wheat - summer maize, 2-year cycle).

fertilization and irrigation in diversified systems are also largely due to crop-specific root traits that enhance resource acquisition (Reich, 2014). For example, in the SpWM (sweet potato-wheat-maize) rotation, sweet potato received the lowest N application of 29.4 kg ha^{-1}, which is in line with local farming practices. This reflects the crop's relatively low N requirements compared to other crops in the rotation and its dependence on phosphorus and potassium for tuber development. In addition, its deep and fibrous roots increase water-use efficiency and reduce irrigation needs (Sokolow et al., 2019). In our biennial four-crop rotation of ryegrass-sorghum-wheat-maize, ryegrass received a relatively low fertilization rate of 118.5 kg ha^{-1}, due to its extensive fine root system that efficiently uses N (Bollam et al., 2021). This efficient use of N contrasts with the high N requirements of wheat and maize for grain yield. Similarly, the high specific root length and root length density of soybean and peanut roots optimize water and nutrient uptake in the topsoil (Porte et al., 2023). Sorghum's deep-rooting ability allows for efficient water extraction from subsoil layers (Lamb et al., 2022). The reduction of synthetic N fertilization and irrigation in these diversified systems leads to potentially lower nitrification and denitrification intensities, ultimately resulting in reducing N_2O emissions (Liu et al., 2011; Shcherbak et al., 2014). Therefore, root traits play a critical role in the success of diversified crop rotations with reduced fertilization and irrigation, making them key factors in lowering N_2O emissions (Abalos et al., 2018). Despite the reduction in fertilization and irrigation, the overall diversified rotation systems produced yields equal to or greater than conventional wheat-maize rotations (Yang et al., 2024).

In addition to synthetic fertilizer N rates, other factors strongly contributed to the differences in N_2O emissions between crop rotations (Fig. 6). This is clearly illustrated by the discrepancy between cumulative N_2O emissions and EFs for the different crop rotations (Fig. 3). In particular, the rotations with the legume soybean or sweet potato showed a reduction in N_2O emissions when compared to the traditional WM rotation, both for cumulative N_2O emissions and for EFs. Various mechanisms can explain the lower emissions of these diversified rotations. For example, the N_2O reductions can be attributed to the differences in root structure—the mix of shallow and deep roots, for example, soybean, sweet potato, wheat, and maize—enhancing soil aggregation, porosity, aeration, and drainage (Nyawade et al., 2019; Shah et al., 2021). Subsequent rotational crops following soybean and sweet potato, like winter wheat, also benefited from these improved soil physical conditions, resulting in increased nutrient uptake in the same field experiment (Yang et al., 2024) and thus reduced N loss and N_2O emissions. Another mechanism is that these crops can release a variety of organic compounds, including sugars, organic acids, amino acids, and secondary metabolites (Bais et al., 2006; Jing et al., 2023). These low weight molecular compounds contribute to the formation of SOC

(Fig. S5, Jones et al., 2009). In sandy loam soils such as those at our sites, this can lead to an increase in mineral-associated organic C that is less accessible for microbial degradation (Just et al., 2023), creating less favourable conditions for denitrification (Fig. S6, de Figueiredo et al., 2018). Furthermore, soybean and sweet potato rotations resulted in higher C/N ratios compared to WM rotations due to increased SOC and reduced synthetic fertilization (Fig. S5D). In this high soil C/N scenario, microbial decomposition of organic matter and N mineralization slow down (Bengtsson et al., 2003; Springob and Kirchmann, 2003), which in turn may reduce denitrification, resulting in lower N_2O emissions. Klemedtsson et al. (2005) also reported a negative correlation between soil C/N ratio and N_2O emissions. This seems to be supported by the observed negative relationships between SOC, soil C/N ratio, and the relative abundance of denitrifying microbes and N_2O emissions (Fig. 6, S5).

The spring maize and peanut-based crop rotations had the highest EFs in all rotations (Fig. 4B), indicating higher N_2O emissions per unit of N fertilizer. Introducing spring maize into traditional maize-wheat rotations has been adopted due to its yield benefits over summer maize (Gao et al., 2018). However, spring maize was planted in early spring with cooler temperatures and higher soil moisture levels, which could lead to increased N_2O emissions by enhancing denitrification and by the lower crop N uptake during the initial growth stages. In our peanut-based rotation, N fertilization was applied in two splits for peanut, at 75 and 82 kg N ha^{-1}, respectively (Table S2). Such suboptimal fertilization practices could lead to increased N_2O emissions, compromising peanuts' natural ability to fix atmospheric N, especially when compared to soybean-based cropping systems (Fig. 5A). This is supported by Wang et al. (2016), who identified a significant negative correlation between the level of N fixation by peanut rhizobia and the amount of fertilizer N applied. Additionally, Liu et al. (2023) indicates that optimal biological N fixation in peanut is achieved with a N application of 15 kg ha^{-1}. Furthermore, the high DOC concentration in the peanut-based rotation may have stimulated denitrification (Fig. S5).

4.3. Reductions in N_2O emissions associated with changes in prokaryotic community structure

Shifts in the microbial communities involved in nitrification and denitrification processes helped explain the N_2O reductions achieved in diverse rotations. Compared to WM rotations, an increase in bacterial α-diversity was noted in both legume and sweet potato-based rotations (Yang et al., 2024), particularly with shifts in specific bacterial and archaeal groups (Fig. 5B). The increase in ammonia-oxidizing bacteria (*MND1*) and ammonia-oxidizing archaea (*Candidatus Nitrososphaera*) of legume and sweet potato-based rotations, along with a decrease in an unclassified genus within the ammonia-oxidizing archaea Nitrososphaeraceae (Fig. 5B), suggests an optimization of the nitrification process (Leininger et al., 2006; Zhang et al., 2022). This efficiency may imply that the transformation of ammonium is more complete, reducing the concomitant accumulation of ammonium and nitrite, which could promote N_2O by nitrifier denitrification when oxygen concentration is between aerobic and anaerobic (Fig. 5A). The reduction in *Rhodoplanes* and an increase in *Paracoccus* within the denitrification pathway (Fig. 5B) also potentially altered N_2O production. *Rhodoplanes* may be involved in pathways that lead to N_2O generation (Zhang et al., 2022), whereas *Paracoccus* is likely more effective in reducing N_2O to N_2, thus decreasing N_2O emissions as a byproduct (Albertsson et al., 2019). In contrast, the traditional WM rotation, characterized by highest N application (594 kg N ha^{-1}) and intensive irrigation, leads to increased N_2O emissions (Fig. 4A). This scenario is attributed to the increased N levels and reduced soil aeration (Fig. S5), which together creates optimal conditions for denitrifying bacteria (e.g. *Rhodoplanes*). These bacteria are more active in N-rich and anaerobic conditions (Zhang et al., 2022; Fig. 5, 6, S5), leading to higher rates of denitrification and subsequent N_2O emissions.

4.4. Implications for agricultural land use and limitation

This long-term monitoring field experiment highlights the key role of diversified crop rotations in the context of climate-smart agriculture (Liang et al., 2023; Liu et al., 2022). Compared to traditional wheat-maize rotations, diversified rotations on one hand reduce the need for resources such as synthetic fertilizers and irrigation, thereby improving resource efficiency and increasing equivalent yields (Yang et al., 2024). These rotations including legumes and cash crops, also cater to diverse market demands, increasing production for uses like feed and bioenergy, which in turn enhances farmers' incomes. In addition, our study shows that diversified rotations can contribute to environmental benefits by reducing N_2O emissions. From a policy perspective, it is imperative to support and promote diversified crop rotations to maximize their economic and environmental benefits. If appropriately designed, diversified rotations may simultaneously increase SOC and mitigate N_2O emissions, for example when soybean and sweet potato are introduced. Future studies should examine the SOC stock changes and the stability of the SOC pools modified by such rotations. The proper management of N fertilizer rates is also critical to control N_2O emissions, as demonstrated by the EFs associated with peanut-based rotations. Our results also suggest that shifts in specific bacterial and archaeal groups, such as *MND1, Candidatus Nitrososphaera, Rhodoplanes*, and *Paracoccus,* may be highly influential on N_2O emissions within diversified cropping systems. Future research should further investigate how specific microbial communities associated with different crops regulate nitrification and denitrification processes. This could help to identify strategies to enhance N cycling efficiency and reduce N_2O emissions, contributing to more effective and sustainable crop rotation designs. Overall, this research improves our understanding of diversified crop rotations, offering important insights for policies and agricultural strategies that support environmental sustainability and food security. A limitation of this study is the inability to fully isolate the effects of fertilization and irrigation from effects of crop rotation. While reduced inputs correlate with reduced N_2O emissions, the lack of strict control over these variables limits definitive attribution to crop rotation alone. Future studies should include consistent management practices across systems to draw clearer conclusions.

5. Conclusion

Our long-term field monitoring experiment reveals that diversified crop rotations can reduce cumulative N_2O emissions by 23 % to 49 % compared to conventional wheat-maize rotation, largely due to the reduced need for synthetic N fertilization and irrigation. Beyond these factors, the reduction in N_2O emissions in rotations involving soybean and sweet potato was also supported by an increase in SOC and soil C/N ratio. However, compared with the conventional wheat-maize rotation, the spring maize- and peanut-based rotation systems had the two highest EFs due to low crop N uptake at initial development stages and improper fertilization strategy, respectively. A key finding of this study is the significant role of prokaryotic community composition in influencing N_2O emissions. The changes in soil microbiota, particularly the increase in ammonia-oxidizing bacteria *MND1* and archaea *Candidatus Nitrososphaera* in legume and sweet potato rotations, along with shifts in denitrifying microbes in various rotations (notably a decrease in *Rhodoplanes* and an increase in *Paracoccus*), was found to contribute substantially to the reduction in emissions. This research underscores the importance of crop rotation diversity in lowering agricultural N_2O emissions and highlights the potential of integrating such practices for more sustainable farming. The findings also emphasize the need for managing soil microbiota as part of effective agricultural strategies aimed at reducing greenhouse gas emissions.

CRediT authorship contribution statement

Mingming Zong: Writing – original draft, Software, Formal analysis. **Xiaolin Yang:** Writing – review & editing, Writing – original draft, Supervision, Methodology, Data curation, Conceptualization. **Alberto Sanz-Cobena:** Writing – review & editing, Validation. **Uffe Jørgensen:** Writing – review & editing, Validation, Investigation. **Klaus Butterbach-Bahl:** Writing – review & editing, Validation, Methodology, Funding acquisition, Conceptualization. **Diego Abalos:** Writing – review & editing, Validation, Methodology, Funding acquisition, Conceptualization.

Declaration of competing interest

The authors declare that they have no known competing financial interests or personal relationships that could have appeared to influence the work reported in this paper.

Acknowledgements

We thank J.X., J.Z., N.Q., P.H., and F.L. from China Agricultural University for field work contributions and Dr. Y.S. for assisting with the analysis of soil microbial communities. This work was financed jointly by the National Natural Science Foundation of China (No. 32071975 and No.52239002) and China Scholarship Council (CSC NO: 202107030005). DA thanks the Danish Council for Independent Research for funding via a Sapere Aude—DFF Research Leader grant, project "Redefining a plant ideotype to reduce nitrogen pollution" (Grant No. 1051–00060B). KBB received additional funding via the Pioneer Center for Landscape Research in Sustainable Agricultural Futures (Land-CRAFT), DNRF Grant P2.

Supplementary materials

Supplementary material associated with this article can be found, in the online version, at doi:10.1016/j.agrformet.2024.110370.

Data availability

Data will be made available on request.

References

Abalos, D., Brown, S.E., Vanderzaag, A.C., Gordon, R.J., Dunfield, K.E., Wagner-Riddle, C., 2016. Micrometeorological measurements over 3 years reveal differences in N_2O emissions between annual and perennial crops. Glob. Change Biol. 22, 1244–1255. https://doi.org/10.1111/gcb.13137.

Abalos, D., Recous, S., Butterbach-Bahl, K., De Notaris, C., Rittl, T.F., Topp, C.F.E., Petersen, S.O., Hansen, S., Bleken, M.A., Rees, R.M., Olesen, J.E., 2022a. A review and meta-analysis of mitigation measures for nitrous oxide emissions from crop residues. Sci. Total. Environ. 828, 154388. https://doi.org/10.1016/j.scitotenv.2022.154388.

Abalos, D., Rittl, T.F., Recous, S., Thiébeau, P., Topp, C.F.E., van Groenigen, K.J., Butterbach-Bahl, K., Thorman, R.E., Smith, K.E., Ahuja, I., Olesen, J.E., Bleken, M.A., Rees, R.M., Hansen, S., 2022b. Predicting field N_2O emissions from crop residues based on their biochemical composition: a meta-analytical approach. Sci. Total Environ. 812, 152532. https://doi.org/10.1016/j.scitotenv.2021.152532.

Abalos, D., van Groenigen, J.W., De Deyn, G.B., 2018. What plant functional traits can reduce nitrous oxide emissions from intensively managed grasslands? Glob. Change Biol. 24, e248–e258. https://doi.org/10.1111/gcb.13827.

Albertsson, I., Sjöholm, J., ter Beek, J., Watmough, N.J., Widengren, J., Ädelroth, P., 2019. Functional interactions between nitrite reductase and nitric oxide reductase from *Paracoccus denitrificans*. Sci. Rep. 9, 17234. https://doi.org/10.1038/s41598-019-53553-z.

Aßhauer, K.P., Wemheuer, B., Daniel, R., Meinicke, P., 2015. Tax4Fun: predicting functional profiles from metagenomic 16S rRNA data. Bioinformatics 31, 2882–2884. https://doi.org/10.1093/bioinformatics/btv287.

Bais, H.P., Weir, T.L., Perry, L.G., Gilroy, S., Vivanco, J.M., 2006. The Role of root exudates in rhizosphere interactions with plants and other organisms. Annu. Rev. Plant Biol. 57, 233–266. https://doi.org/10.1146/annurev.arplant.57.032905.105159.

Beillouin, D., Ben-Ari, T., Malézieux, E., Seufert, V., Makowski, D., 2021. Positive but variable effects of crop diversification on biodiversity and ecosystem services. Glob. Change Biol. 27, 4697–4710. https://doi.org/10.1111/gcb.15747.

Bengtsson, G., Bengtson, P., Månsson, K.F., 2003. Gross nitrogen mineralization-, immobilization-, and nitrification rates as a function of soil C/N ratio and microbial activity. Soil Biol. Biochem. 35, 143–154. https://doi.org/10.1016/S0038-0717(02)00248-1.

Bokulich, N.A., Subramanian, S., Faith, J.J., Gevers, D., Gordon, J.I., Knight, R., Mills, D. A., Caporaso, J.G., 2013. Quality-filtering vastly improves diversity estimates from Illumina amplicon sequencing. Nat. Methods 10, 57–59. https://doi.org/10.1038/nmeth.2276.

Bollam, S., Romana, K.K., Rayaprolu, L., Vemula, A., Das, R.R., Rathore, A., Gandham, P., Chander, G., Deshpande, S.P., Gupta, R., 2021. Nitrogen use efficiency in sorghum: exploring native variability for traits under variable N-regimes. Front. Plant. Sci. 12. https://doi.org/10.3389/fpls.2021.643192.

Bremner, J.M., 1965. Inorganic forms of nitrogen, in: methods of soil analysis. John Wiley Sons,. Ltd 1179–1237. https://doi.org/10.2134/agronmonogr9.2.c33.

Bremner, J.M., Shaw, K., 1958. Denitrification in soil. I. methods of investigation. J. Agric. Sci. 51, 22–39. https://doi.org/10.1017/S0021859600032767.

Caporaso, J.G., Kuczynski, J., Stombaugh, J., Bittinger, K., Bushman, F.D., Costello, E.K., Fierer, N., Peña, A.G., Goodrich, J.K., Gordon, J.I., Huttley, G.A., Kelley, S.T., Knights, D., Koenig, J.E., Ley, R.E., Lozupone, C.A., McDonald, D., Muegge, B.D., Pirrung, M., Reeder, J., Sevinsky, J.R., Turnbaugh, P.J., Walters, W.A., Widmann, J., Yatsunenko, T., Zaneveld, J., Knight, R., 2010. QIIME allows analysis of high-throughput community sequencing data. Nat. Methods 7, 335–336. https://doi.org/10.1038/nmeth.f.303.

Chen, H.H., Li, X.C., Hu, F., Shi, W., 2013. Soil nitrous oxide emissions following crop residue addition: a meta-analysis. Glob. Change. Biol. 19, 2956–2964. https://doi.org/10.1111/gcb.12274.

Clayton, H., Arah, J.M., Smith, K.A., 1994. Measurement of nitrous oxide emissions from fertilized grassland using closed chambers. J. Geophys. Res 99. https://doi.org/10.1029/94JD00218, 16599–16607.

Cui, F., Yan, G.X., Zhou, Z.X., Zheng, X.H., Deng, J., 2012. Annual emissions of nitrous oxide and nitric oxide from a wheat–maize cropping system on a silt loam calcareous soil in the North China Plain. Soil Biol. Biochem. 48, 10–19. https://doi.org/10.1016/j.soilbio.2012.01.007.

Cui, Z.L., Chen, X.P., Zhang, F.S., 2010. Current nitrogen management status and measures to improve the intensive wheat–maize system in China. AMBIO 39, 376–384. https://doi.org/10.1007/s13280-010-0076-6.

de Figueiredo, C.C., de Oliveira, A.D., dos Santos, I.L., Ferreira, E.A.B., Malaquias, J.V., de Sá, M.A.C., de Carvalho, A.M., dos Santos, J., de, D.G., 2018. Relationships between soil organic matter pools and nitrous oxide emissions of agroecosystems in the Brazilian Cerrado. Sci. Total Environ. 618, 1572–1582. https://doi.org/10.1016/j.scitotenv.2017.09.333.

Drury, C.F., Reynolds, W.D., Tan, C.S., McLaughlin, N.B., Yang, X.M., Calder, W., Oloya, T.O., Yang, J.Y., 2014. Impacts of 49–51 years of fertilization and crop rotation on growing season nitrous oxide emissions, nitrogen uptake and corn yields. Can. J. Soil. Sci. 94, 421–433. https://doi.org/10.4141/cjss2013-101.

Drury, C.F., Reynolds, W.D., Yang, X., McLaughlin, N.B., Calder, W., Phillips, L.A., 2021. Diverse rotations impact microbial processes, seasonality and overall nitrous oxide emissions from soils. Soil Sci. Soc. Am. J. 85, 1448–1464. https://doi.org/10.1002/saj2.20298.

Edgar, R.C., 2013. UPARSE: highly accurate OTU sequences from microbial amplicon reads. Nat. Methods 10, 996–998. https://doi.org/10.1038/nmeth.2604.

Gao, G.F., Li, P.F., Zhong, J.X., Shen, Z.J., Chen, J., Li, Y.T., Isabwe, A., Zhu, X.Y., Ding, Q.S., Zhang, S., Gao, C.H., Zheng, H.L., 2019. Spartina alterniflora invasion alters soil bacterial communities and enhances soil N2O emissions by stimulating soil denitrification in mangrove wetland. Sci. Total Environ. 653, 231–240. https://doi.org/10.1016/j.scitotenv.2018.10.277.

Gao, Z., Feng, H.Y., Liang, X.G., Zhang, L., Lin, S., Zhao, X., Shen, S., Zhou, L.L., Zhou, S. L., 2018. Limits to maize productivity in the North China Plain: a comparison analysis for spring and summer maize. Field Crops Res 228, 39–47. https://doi.org/10.1016/j.fcr.2018.08.022.

Garnier, J., Casquin, A., Mercier, B., Martinez, A., Gréhan, E., Azougui, A., Bosc, S., Pomet, A., Billen, G., Mary, B., 2024. Six years of nitrous oxide emissions from temperate cropping systems under real-farm rotational management. Agric. For. Meteorol. 354, 110085. https://doi.org/10.1016/j.agrformet.2024.110085.

Goodfellow, M., 2012. Bergey's manual® of systematic bacteriology. No. Title 5, 376. https://doi.org/10.1007/978-0-387-68233-4.

Griffis, T.J., Chen, Z., Baker, J.M., Wood, J.D., Millet, D.B., Lee, X., Venterea, R.T., Turner, P.A., 2017. Nitrous oxide emissions are enhanced in a warmer and wetter world. Proc. Natl. Acad. Sci. 114, 12081–12085. https://doi.org/10.1073/pnas.1704552114.

Grossman, R.B., Reinsch, T.G., 2002. Bulk Density and Linear extensibility, in: Methods of Soil Analysis. John Wiley & Sons, Ltd, pp. 201–228. https://doi.org/10.2136/sssabookser5.4.c9.

Harris, D., Horwáth, W.R., van Kessel, C., 2001. Acid fumigation of soils to remove carbonates prior to total organic carbon or CARBON-13 isotopic analysis. Soil Sci. Soc. Am. J. 65, 1853–1856. https://doi.org/10.2136/sssaj2001.1853.

Harter, J., Krause, H.-M., Schuettler, S., Ruser, R., Fromme, M., Scholten, T., Kappler, A., Behrens, S., 2014. Linking N_2O emissions from biochar-amended soil to the structure and function of the N-cycling microbial community. ISME J 8, 660–674. https://doi.org/10.1038/ismej.2013.160.

Hillel, D., 1980. Introduction to Soil Physics. Academic, San Diego, California, pp. 9–12.

International Journal of Systematic and Evolutionary Microbiology. Available online: https://www.microbiologyresearch.org/content/journal/ijsem (accessed on 11 September 2024).
IPCC, 2021. Climate change, 2021. The physical Science basis. Contribution of Working Group I to the Sixth Assessment Report of the Intergovernmental Panel On Climate Change. Cambridge University Press, Oxford, pp. 7–125.
IPCC, 2019. Refinement to the 2006 IPCC Guidelines for National Greenhouse Gas Inventories. Switzerland. https://www.ipcc-nggip.iges.or.jp/public/2019rf/vol4.html.
Jiang, S., Xing, Y.J., Liu, G.C., Hu, C., Wang, X.C., Yan, G.Y., Wang, Q.G., 2021. Changes in soil bacterial and fungal community composition and functional groups during the succession of boreal forests. Soil Biol. Biochem. 161, 108393. https://doi.org/10.1016/j.soilbio.2021.108393.
Jing, W., Lei, W., Jie, Y., Cong, X., Hui, Z., Meng, Z., Peng, Z., Xiaoya, Z., Zhonghou, T., Jidong, W., Yongchun, Z., 2023. Distinct characteristics of the bacterial community in the rhizosphere soils of sweet potato storage roots and fibrous roots following long-term fertilization. Appl. Soil Ecol. 191, 105053. https://doi.org/10.1016/j.apsoil.2023.105053.
Johnson, J.M.F., Archer, D., Barbour, N., 2010. Greenhouse gas emission from contrasting management scenarios in the Northern Corn Belt. Soil Sci. Soc. Am. J. 74, 396–406. https://doi.org/10.2136/sssaj2009.0008.
Jones, D.L., Nguyen, C., Finlay, R.D., 2009. Carbon flow in the rhizosphere: carbon trading at the soil–root interface. Plant Soil 321, 5–33. https://doi.org/10.1007/s11104-009-9925-0.
Ju, X.T., Xing, G.X., Chen, X.P., Zhang, S.L., Zhang, L.J., Liu, X.J., Cui, Z.L., Yin, B., Christie, P., Zhu, Z.L., Zhang, F.-S., 2009. Reducing environmental risk by improving N management in intensive Chinese agricultural systems. Proc. Natl. Acad. Sci. 106, 3041–3046. https://doi.org/10.1073/pnas.0813417106.
Just, C., Armbruster, M., Barkusky, D., Baumecker, M., Diepolder, M., Döring, T.F., Heigl, L., Honermeier, B., Jate, M., Merbach, I., Rusch, C., Schubert, D., Schulz, F., Schweitzer, K., Seidel, S., Sommer, M., Spiegel, H., Thumm, U., Urbatzka, P., Zimmer, J., Kögel-Knabner, I., Wiesmeier, M., 2023. Soil organic carbon sequestration in agricultural long-term field experiments as derived from particulate and mineral-associated organic matter. Geoderma 434, 116472. https://doi.org/10.1016/j.geoderma.2023.116472.
Klemedtsson, L., Von Arnold, K., Weslien, P., Gundersen, P., 2005. Soil CN ratio as a scalar parameter to predict nitrous oxide emissions. Glob. Change Biol. 11, 1142–1147. https://doi.org/10.1111/j.1365-2486.2005.00973.x.
Krupinsky, J.M., Bailey, K.L., McMullen, M.P., Gossen, B.D., Turkington, T.K., 2002. Managing plant disease risk in diversified cropping systems. Agron. J. 94, 198–209. https://doi.org/10.2134/agronj2002.1980.
Lamb, A., Weers, B., McKinley, B., Rooney, W., Morgan, C., Marshall-Colon, A., Mullet, J., 2022. Bioenergy sorghum's deep roots: a key to sustainable biomass production on annual cropland. GCB. Bioen 14, 132–156. https://doi.org/10.1111/gcbb.12907.
Leininger, S., Urich, T., Schloter, M., Schwark, L., Qi, J., Nicol, G.W., Prosser, J.I., Schuster, S.C., Schleper, C., 2006. Archaea predominate among ammonia-oxidizing prokaryotes in soils. Nature 442, 806–809. https://doi.org/10.1038/nature04983.
Li, W.Y., Xiao, Q., Hu, C.S., Liu, B.B., Sun, R.B., 2019. A comparison of the efficiency of different urease inhibitors and their effects on soil prokaryotic community in a short-term incubation experiment. Geoderma 354, 113877. https://doi.org/10.1016/j.geoderma.2019.07.035.
Li, Y., Chen, J., Drury, C.F., Liebig, M., Johnson, J.M.F., Wang, Z.Z., Feng, H., Abalos, D., 2023. The role of conservation agriculture practices in mitigating N_2O emissions: a meta-analysis. Agron. Sustain. Dev. 43, 63. https://doi.org/10.1007/s13593-023-00911-x.
Liang, Z.Y., Xu, Z., Cheng, J.L., Ma, B.W., Cong, W.F., Zhang, C.C., Zhang, F.S., van der Werf, W.W., Groot, J.C.J., 2023. Designing diversified crop rotations to advance sustainability: a method and an application. Sustain. Prod. Consum. 40, 532–544. https://doi.org/10.1016/j.spc.2023.07.018.
Linton, N.F., Ferrari Machado, P.V., Deen, B., Wagner-Riddle, C., Dunfield, K.E., 2020. Long-term diverse rotation alters nitrogen cycling bacterial groups and nitrous oxide emissions after nitrogen fertilization. Soil Biol. Biochem. 149, 107917. https://doi.org/10.1016/j.soilbio.2020.107917.
Liu, C., Plaza-Bonilla, D., Coulter, J.A., Kutcher, H.R., Beckie, H.J., Wang, L., Floc'h, J.-B., Hamel, C., Siddique, K.H.M., Li, L.L., Gan, Y.T., 2022. Chapter Six - Diversifying crop rotations enhance agroecosystem services and resilience. In: Sparks, D.L. (Ed.), Advances in Agronomy. Academic Press, pp. 299–335. https://doi.org/10.1016/bs.agron.2022.02.007.
Liu, C., Wang, K., Meng, S., Zheng, X., Zhou, Z., Han, S., Chen, D., Yang, Z., 2011. Effects of irrigation, fertilization and crop straw management on nitrous oxide and nitric oxide emissions from a wheat–maize rotation field in northern China. Agric. Ecosyst. Environ. 140, 226–233. https://doi.org/10.1016/j.agee.2010.12.009.
Liu, Y., Yan, Z.H., Wang, J.G., Zhao, J.H., Liu, Y.Y., Zou, J., Li, L., Zhang, J.L., Wan, S.B., 2023. Optimizing initial nitrogen application rates to improve peanut (*Arachis hypogaea* L.) biological nitrogen fixation. Agronomy 13, 3020. https://doi.org/10.3390/agronomy13123020.
Lory, S., 2013. The prokaryotes: prokaryotic biology and symbiotic associations. Rosenberg, E., DeLong, EF, Lory, S., Stackebrandt, E., Thompson, F., Eds, pp.359–400.
Louca, S., Parfrey, L.W., Doebeli, M., 2016. Decoupling function and taxonomy in the global ocean microbiome. Science 353, 1272–1277. https://doi.org/10.1126/science.aaf4507.
Ma, B.L., Liang, C., Herath, A., Caldwell, C.D., Smith, D.L., 2023. Canola productivity and carbon footprint under different cropping systems in eastern Canada. Nutr. Cycl. Agroecosyst. 127, 191–207. https://doi.org/10.1007/s10705-023-10294-w.
Mclean, E.o., 1983. Soil pH and lime requirement. Methods of Soil Analysis. John Wiley & Sons, Ltd, pp. 199–224. https://doi.org/10.2134/agronmonogr9.2.2ed.c12.
Meng, Q.F., Sun, Q.Q., Chen, X.P., Cui, Z.L., Yue, S.C., Zhang, F.S., Römheld, V., 2012. Alternative cropping systems for sustainable water and nitrogen use in the North China Plain. Agric. Ecosyst. Environ. 146, 93–102. https://doi.org/10.1016/j.agee.2011.10.015.
Munkholm, L.J., Heck, R.J., Deen, B., 2013. Long-term rotation and tillage effects on soil structure and crop yield. Soil Tillage Res. 127, 85–91. https://doi.org/10.1016/j.still.2012.02.007.
Noemi Cosentino, V.R., Fernandez, P.L., Figueiro Aureggi, S.A., Taboada, M.A., 2012. N_2O emissions from a cultivated mollisol: optimal time of day for sampling and the role of soil temperature. Rev. Bras. Ciênc. Solo. 36, 1814–1819. https://doi.org/10.1590/S0100-06832012000600015.
Nyawade, S.O., Karanja, N.N., Gachene, C.K.K., Gitari, H.I., Schulte-Geldermann, E., Parker, M.L., 2019. Short-term dynamics of soil organic matter fractions and microbial activity in smallholder potato-legume intercropping systems. Appl. Soil. Ecol. 142, 123–135. https://doi.org/10.1016/j.apsoil.2019.04.015.
Oates, L.G., Duncan, D.S., Gelfand, I., Millar, N., Robertson, G.P., Jackson, R.D., 2016. Nitrous oxide emissions during establishment of eight alternative cellulosic bioenergy cropping systems in the North Central United States. GCB Bioen 8, 539–549. https://doi.org/10.1111/gcbb.12268.
Olesen, J.E., Rees, R.M., Recous, S., Bleken, M.A., Abalos, D., Ahuja, I., Butterbach-Bahl, K., Carozzi, M., De Notaris, C., Ernfors, M., Haas, E., Hansen, S., Janz, B., Lashermes, G., Massad, R.S., Petersen, S.O., Rittl, T.F., Scheer, C., Smith, K.E., Thiébeau, P., Taghizadeh-Toosi, A., Thorman, R.E., Topp, C.F.E., 2023. Challenges of accounting nitrous oxide emissions from agricultural crop residues. Glob. Change. Biol. 29, 6846–6855. https://doi.org/10.1111/gcb.16962.
Olsen, S.R., Sommers, L.E, 1982. Phosphorus. In: Page, A.L (Ed.), Methods of Soil Analysis Part 2 Chemical and Microbiological Properties, American Society of Agronomy. Soil Science Society of America, Madison, pp. 403–430.
Pan, S.Y., He, K.H., Lin, K.T., Fan, C., Chang, C.T., 2022. Addressing nitrogenous gases from croplands toward low-emission agriculture. Npj. Clim. Atmosph. Sci. 5, 1–18. https://doi.org/10.1038/s41612-022-00265-3.
Petersen, S.O., Mutegi, J.K., Hansen, E.M., Munkholm, L.J., 2011. Tillage effects on N2O emissions as influenced by a winter cover crop. Soil Biol. Biochem. 43, 1509–1517. https://doi.org/10.1016/j.soilbio.2011.03.028.
Porte, A., Bellingrath-Kimura, S.D., Schmidtke, K., 2023. Root development and subsoil 15N-labelled N uptake in soybean (Glycine max (L.) Merr.). J. Soil Sci. Plant Nutr. 23, 6257–6272. https://doi.org/10.1007/s42729-023-01482-2.
R Development Core Team, 2020. R: a language and environment for statistical computing. R. Found. Statist. Comp.
Reay, D.S., Davidson, E.A., Smith, K.A., Smith, P., Melillo, J.M., Dentener, F., Crutzen, P. J., 2012. Global agriculture and nitrous oxide emissions. Nat. Clim. Change 2, 410–416. https://doi.org/10.1038/nclimate1458.
Reich, P.B., 2014. The world-wide 'fast–slow' plant economics spectrum: a traits manifesto. J. Ecol. 102, 275–301. https://doi.org/10.1111/1365-2745.12211.
Rohe, L., Apelt, B., Vogel, H.-J., Well, R., Wu, G.-M., Schlüter, S., 2021. Denitrification in soil as a function of oxygen availability at the microscale. Biogeosciences 18, 1185–1201. https://doi.org/10.5194/bg-18-1185-2021.
Schlüter, S., Lucas, M., Grosz, B., Ippisch, O., Zawallich, J., He, H., Dechow, R., Kraus, D., Blagodatsky, S., Senbayram, M., Kravchenko, A., Vogel, H.-J., Well, R., 2024. The anaerobic soil volume as a controlling factor of denitrification: a review. Biol. Fertil. Soils. https://doi.org/10.1007/s00374-024-01819-8.
Shah, K.K., Modi, B., Pandey, H.P., Subedi, A., Aryal, G., Pandey, M., Shrestha, J., 2021. Diversified crop rotation: an approach for sustainable agriculture production. Adv. Agric. 2021, 8924087. https://doi.org/10.1155/2021/8924087.
Shcherbak, I., Millar, N., Robertson, G.P., 2014. Global metaanalysis of the nonlinear response of soil nitrous oxide (N_2O) emissions to fertilizer nitrogen. Proc. Natl. Acad. Sci. 111, 9199–9204. https://doi.org/10.1073/pnas.1322434111.
Shi, M., Li, J., Zhou, Q., Wang, G., Zhang, W., Zhang, Z., Gao, Y., Yan, S., 2020. Interactions between elevated CO_2 levels and floating aquatic plants on the alteration of bacterial function in carbon assimilation and decomposition in eutrophic waters. Water Res 171, 115398. https://doi.org/10.1016/j.watres.2019.115398.
Sokolow, J., Kennedy, G., Attwood, S., 2019. Managing Crop tradeoffs: a methodology for comparing the water footprint and nutrient density of crops for food system sustainability. J. Clean Prod. 225, 913–927. https://doi.org/10.1016/j.jclepro.2019.03.056.
Springob, G., Kirchmann, H., 2003. Bulk soil C to N ratio as a simple measure of net N mineralization from stabilized soil organic matter in sandy arable soils. Soil Biol. Biochem. 35, 629–632. https://doi.org/10.1016/S0038-0717(03)00052-X.
Taghizadeh-Toosi, A., Janz, B., Labouriau, R., Olesen, J.E., Butterbach-Bahl, K., Petersen, S.O., 2021. Nitrous oxide emissions from red clover and winter wheat residues depend on interacting effects of distribution, soil N availability and moisture level. Plant Soil 466, 121–138. https://doi.org/10.1007/s11104-021-05030-8.
Tallec, T., Bigaignon, L., Delon, C., Brut, A., Ceschia, E., Mordelet, P., Zawilski, B., Granouillac, F., Claverie, N., Fieuzal, R., Lemaire, B., Le Dantec, V., 2022. Dynamics of nitrous oxide emissions from two cropping systems in southwestern France over 5 years: cross impact analysis of heterogeneous agricultural practices and local climate variability. Agric. For. Meteorol. 323, 109093. https://doi.org/10.1016/j.agrformet.2022.109093.
Tan, Y.C., Xu, C., Liu, D.X., Wu, W.L., Lal, R., Meng, F.Q., 2017. Effects of optimized N fertilization on greenhouse gas emission and crop production in the North China Plain. Field Crops Res 205, 135–146. https://doi.org/10.1016/j.fcr.2017.01.003.

Tiemann, L.K., Grandy, A.S., Atkinson, E.E., Marin-Spiotta, E., McDaniel, M.D., 2015. Crop rotational diversity enhances belowground communities and functions in an agroecosystem. Ecol. Lett. 18, 761–771. https://doi.org/10.1111/ele.12453.

Vance, E.D., Brookes, P.C., Jenkinson, D.S., 1987. An extraction method for measuring soil microbial biomass C. Soil Biol. Biochem. 19, 703–707. https://doi.org/10.1016/0038-0717(87)90052-6.

Vos, P., Garrity, G., Jones, D., Krieg, N.R., Ludwig, W., Rainey, F.A., Schleifer, K.-H., Whitman, W.B., 2011. Bergey's Manual of Systematic Bacteriology: Volume 3: The Firmicutes. Springer Science & Business Media.

Wang, C., Zheng, Y.M., Shen, P., Zheng, Y.P., Wu, Z., Sun, X., Yu, T., Feng, H., 2016. Determining N supplied sources and N use efficiency for peanut under applications of four forms of N fertilizers labeled by isotope ^{15}N. J. Integr. Agric. 15, 432–439. https://doi.org/10.1016/S2095-3119(15)61079-6.

Wang, Y.Y., Hu, C.S., Ming, H., Zhang, Y.M., Li, X.X., Dong, W.X., Oenema, O., 2013. Concentration profiles of CH_4, CO_2 and N_2O in soils of a wheat–maize rotation ecosystem in North China Plain, measured weekly over a whole year. Agric. Ecosyst. Environ. 164, 260–272. https://doi.org/10.1016/j.agee.2012.10.004.

Xiao, H., van Es, H.M., Amsili, J.P., Shi, Q.Q., Sun, J.B., Chen, Y.Q., 2022. Lowering soil greenhouse gas emissions without sacrificing yields by increasing crop rotation diversity in the North China Plain. Field Crops Res 276, 108366. https://doi.org/10.1016/j.fcr.2021.108366.

Yang, X.L., Xiong, J.R., Du, T.S., Ju, X.T., Gan, Y.T., Li, S.E., Xia, L.L., Shen, Y.J., Pacenka, S., Steenhuis, T.S., Siddique, K.H.M., Kang, S.Z., Butterbach-Bahl, K., 2024. Diversifying crop rotation increases food production, reduces net greenhouse gas emissions and improves soil health. Nat. Commun. 15, 198. https://doi.org/10.1038/s41467-023-44464-9.

Yuan, Z.J., Shen, Y.J., 2013. Estimation of agricultural water consumption from meteorological and yield data: a case study of Hebei, North China. Plos One 8, e58685. https://doi.org/10.1371/journal.pone.0058685.

Zhang, H.Y., Shi, Y.C., Dong, Y.X., Lapen, D.R., Liu, J.H., Chen, W., 2022. Subsoiling and conversion to conservation tillage enriched nitrogen cycling bacterial communities in sandy soils under long-term maize monoculture. Soil Tillage Res 215, 105197. https://doi.org/10.1016/j.still.2021.105197.

Zheng, X.H., Mei, B.L., Wang, Y.H., Xie, B.H., Wang, Y.S., Dong, H.B., Xu, H., Chen, G.X., Cai, Z.C., Yue, J., Gu, J.X., Su, F., Zou, J.W., Zhu, J.G., 2008. Quantification of N_2O fluxes from soil–plant systems may be biased by the applied gas chromatograph methodology. Plant Soil 311, 211–234. https://doi.org/10.1007/s11104-008-9673-6.

Zong, M., Manevski, K., Liang, Z., Abalos, D., Jabloun, M., Lærke, P.E., Jørgensen, U., 2024. Diversifying maize rotation with other industrial crops improves biomass yield and nitrogen uptake while showing variable effects on nitrate leaching. Agric. Ecosyst. Environ 371, 109091. https://doi.org/10.1016/j.agee.2024.109091.